Ionic complexes of poly(γ-glutamic acid) with alkyltrimethylphosphonium surfactants

Ana Gamarra[a], Antxon Martínez de Ilarduya[a], Marc Vives[b], Jordi Morató[b], Sebastián Muñoz-Guerra[a]*

[a]*Departament d'Enginyeria Química, Universitat Politècnica de Catalunya, ETSEIB, Diagonal 647, Barcelona 08028, Spain.*

[b]*Health and Environmental Microbiology Lab & UNESCO Chair on Sustainability, Universitat Politècnica de Catalunya, ESEIAAT, Edifici Gaia, Pg. Ernest Lluch/Rambla Sant Nebridi, Terrassa 08222, Spain*

E-mail: sebastian.munoz@upc.edu

Abstract: A series of ionic complexes with a comb-like architecture and a nearly stoichiometric composition were prepared from bacterial poly(γ,DL-glutamic acid) (PGGA) and alkyltrimethyl phosphonium bromides (*n*ATMP·Br) bearing long linear alkyl chains with even numbers of carbon atoms (*n*) ranging from 12 to 22. The *n*ATMP·PGGA complexes were non-water soluble but readily soluble in organic solvents, and they displayed a high thermal stability. Combined DSC and XRD studies revealed that these complexes adopted an amphiphilic layered structure with the polypeptide chain and the alkyl chain separated in two differentiated phases with a nanoperiodicity that increased steadily with the length of the alkyl chain. The paraffinic phase was found to be partially crystallized in an extent that decreased with *n*, so that complexes with *n* = 12 and 14 did not show any sign of crystallinity whereas those with *n* from 16 to 22 showed crystalline melting in the ~30-70 ºC range. The structural transitions taking place by temperature effects were characterized by simultaneous SAXS/WAXS using synchrotron radiation at real time. In all cases, a shortening of the layer periodicity occurred upon heating with recovering of the initial structure after cooling. *n*ATMP·PGGA with *n* ≤ 16 showed strong antimicrobial activity against both *E. coli* and *S. aureus,* a property that could be related to the weak dissociation of the complexes happening upon incubation in water. The structure and properties of these complexes where comparatively discussed taking as reference their analog complexes made from PGGA and alkyltrimethylammonium bromides already studied by us.

1. Introduction

Poly(γ-glutamic acid) (PGGA) is an emerging biopolymer that attracts plenty of research due to its outstanding properties such as water affinity, biodegradability and biocompatibility, in addition to be functionalized [1]. Nevertheless, the industrial production and commercial spreading of this poly(γ-peptide) becomes seriously limited by its poor stability in humid environments and its incapacity for being processed. A diversity of modifications of PGGA consisting mainly on esterification [1–3] or amidation [1,4,5] of the carboxylic side groups have been reported as convenient approaches to render non-water soluble polymers able to be processed by applying either humid or dried methods. Nevertheless, the covalent modification of PGGA is a tricky procedure that usually implies long reaction times as well as the use of large amounts of solvents and reagents that in most of cases are of unsatisfactory sustainability.

Coupling of carboxylic polypeptides with cationic surfactants has proven to be a very convenient route to produce comb-like ionic complexes that are resistant to water and well stable to heating, and that tend to be self-assembled in supramolecular structures of both academic and practical interest [6]. Such complexes are readily prepared by just mixing aqueous solutions of the polyacid and the surfactant, and they are usually made of stoichiometric or nearly stoichiometric ratios of the two components. Around ten years ago we described for the first time the ionic complexes made of PGGA, either nearly racemic [7] or largely enriched in the D-enantiomer [8], and alkyltrimethylammonium surfactants (*n*ATMA) bearing linear alkyl chains with numbers of carbons (*n*) from 12 to 22. It was then ascertained by different methods that these complexes (*n*ATMA·PGGA) adopted an amphiphilic layered structure consisting of two separated phases, a hydrophilic one lodging the polypeptide chains and a hydrophobic other integrated by the alkyl side chains. This structure was found to be highly sensitive to temperature showing reversible dimensional changes upon heating or cooling within the 20-70 ºC range. The potential of these complexes as thermoresponsive carriers for

hydrophobic active compound has been repeatedly claimed [8], and their capacity for improving the compatibility of PGGA and nanoclays in layered nanocomposites has been clearly demonstrated [9]. More recently ionic complexes of PGGA of varying stoichiometry have been made using alkanoylcholines derived from fatty acids as counterions [10]. These entirely bio-based complexes are also arranged in a layered structure with features similar to those found for *n*ATMA·PGGA complexes. Furthermore non-stoichiometric choline derived complexes were used for building biodegradable nanoparticles of 50–100 nm which were able to charge efficiently and deliver under control different kind of drugs of therapeutic interest [11].

In this study we wish to report on comb-like ionic complexes made by coupling racemic PGGA with alkyltrimethylphosphonium soaps, abbreviated *n*ATMP·PGGA where *n* stands for the number of carbon atoms contained in the linear alkyl chain taking even values from 12 up to 22. The structure and thermotropic behavior of the organophosphonium salts (*n*ATMP·Br) used in this work have been examined in detail in a recently published paper [12]. Two main reasons among others have encouraged us to undertake the present study. Firstly it is of fundamental interest to know if the replacement of nitrogen by phosphorous, which is a much more bulky atom, may have significant influence on the ionic PGGA-surfactant complexes regarding essential aspects as crystallizability, formation of the layered structure and response to heating effects. Secondly alkyltrimethylphosphonium compounds are known to be much more resistant to temperature than their ammonium analogs [13] and also to exert a more strong biocide activity [14]. These properties will be relevant for the behavior of their complexes with PGGA which should be expected therefore to show high thermal stability and intense antimicrobial activity, both properties being of interest for the potential utilization of *n*ATMP·PGGA as extruded films in active coating and packaging applications.

2. Experimental section

2.1. Materials

The sodium salt of poly(γ-glutamic acid) (Na·PGGA) sample used in this work was kindly supplied by Dr. Kubota of Meiji. Co. (Japan). It was obtained by biosynthesis with a weight-average molecular weight of ~300,000 Da and a D:L enantiomeric ratio of 59:41. Alkyltrimethylphosphonium surfactants (*n*ATMP·Br for even values of *n* from 12 to 22) were synthetized by reaction of the corresponding 1-bromoalkanes with trimethylphosphine in toluene solution following a procedure described previously by us [12].

2.2. Measurements

FTIR spectra were recorded from powder samples within the 4000-600 cm^{-1} interval on a FTIR Perkin Elmer Frontier spectrophotometer provided with a universal ATR sampling accessory for the examination of solid samples. ^{1}H and ^{13}C NMR spectra were recorded on a Bruker AMX-300 NMR instrument using TMS as internal reference. The spectra were registered at 300.1 MHz for ^{1}H NMR and at 75.5 MHz for ^{13}C NMR from samples dissolved in deuterated chloroform. Thermogravimetric analyses were performed on a Mettler-Toledo TGA/DSC 1 Star System under a nitrogen flow of 20 $mL \cdot min^{-1}$ at a heating rate of 10 $ºC \cdot min^{-1}$ using sample weights of 10-15 mg. Calorimetric measurements were performed with a Perkin-Elmer DSC 8000 instrument calibrated with indium and zinc. Sample weights of about 2-5 mg were subjected to heating-cooling cycles at a rate of 10 $ºC \cdot min^{-1}$ within the temperature range of -30 to 120 ºC under a nitrogen atmosphere. Optical microscopy was carried out on an Olympus BX51 polarizing optical microscope equipped with a digital camera. Samples for observation were prepared by casting 5% (v/v) chloroform solutions of *n*ATMP·PGGA complexes on a microscope glass coverslip and the dried film covered with another slide. Real time X-ray diffraction studies were carried out using X-ray synchrotron radiation at the BL11 beamline (NCD, Non-Crystalline Diffraction) of ALBA facilities (Cerdanyola del Vallès, Barcelona). Both

SAXS and WAXS were taken simultaneously from powder samples subjected to heating-cooling cycles at a rate of 10 ºC·min^{-1}. The radiation energy employed corresponded to a 0.10 nm wavelength, and spectra were calibrated with silver behenate (AgBh) and Cr_2O_3 for SAXS and WAXS, respectively.

The antimicrobial activity of *n*ATMP·PGGA complexes was tested in vivo against both Gram-negative *Escherichia coli* ATCC 9001 and Gram-positive *Staphylococcus aureus* in liquid culture media over time. Bacterial cultures were incubated in TSA for 24 h at 37 ºC and then transferred to a TSB (Triptic Soy Broth) medium where they were left to grow for 24 h at 37 ºC to produce the corresponding subcultures. Prior to the assay a *loopful* of each strain was transferred to 10 mL of fresh TSB and incubated at 37 ºC for 18 h to assess their exponential growth. Cultures were then diluted to obtain the desired concentration which was fixed at $2.05 \cdot 10^9$ and $2.1 \cdot 10^8$ cfu·mL^{-1} for *E. coli* and *S. aureus*, respectively, as estimated by optical density measurements at 600 nm. Polymer specimens for the assays were squares of approximately 1x1 cm^2 cut from thin films of *n*ATMP·PGGA complexes that had been prepared by casting and then heated under vacuum. For testing their antimicrobial activity, squares were immersed into 10 mL of TSB with 100 μL of each microorganism added and incubated at 37 ºC during scheduled times. For quantification, 100 μL aliquots were removed from the suspension at selected periods of time, successively diluted with peptone buffer solution and plated in duplicates in Petri dishes in a TSA culture medium. Colonies were counted after incubation at 37 °C for 24 h. Counts were performed in triplicates.

Antimicrobial activity of *n*ATMP·PGGA films was also estimated by a second method by following the growth curve of each microorganism in the presence of compounds released from the complexes upon incubation. Colony counting was made by photometric measurement using a Tecan's Magellan™ instrument. Firstly, each film was immersed in tubes containing 10 mL of TSB at pH 5 or 7 and incubated for 5 days at 4 ºC. Then 200 µL of the supernatant liquid was

transferred to ELISA plates containing 2 µL of *E. coli* or *S. aureus* and incubated at 37 °C for 24 h under agitation. Measurements were made at λ = 490 nm at regular periods of time over the whole incubation period.

2.3. Preparation of *n*ATMP·PGGA complexes

The complexes made from PGGA and *n*ATMP surfactants were prepared following the methodology initially reported by Ponomarenko et al. [15] for the synthesis of complexes made from charged poly(α-aminoacids) and ionic surfactants, and that was later applied by us for coupling either PGGA [7,8] or polyuronic acids [16,17] with quaternary ammonium salts bearing long alkyl chains. In brief, an aqueous solution of the *n*ATMP·Br salt was added dropwise to a solution of Na·PGGA in water under stirring at a temperature between 25 and 65 ºC depending on the surfactant water solubility. After several hours of standing a white precipitate appeared which was isolated by centrifugation, repeatedly washed with water, and finally dried under vacuum for at least 48 h. All complexes were collected as white to pale non-hygroscopic powders.

3. Results and discussion

3.1. Synthesis and chemical characterization of *n*ATMP·PGGA complexes.

The coupling reaction between Na·PGGA and *n*ATMP·Br leading to *n*ATMP·PGGA ionic complexes with *n* even values from 12 to 22 is depicted in Scheme I. The reaction conditions used and the results obtained for the six complexes prepared in this work are compared in Table 1. The temperature used for mixing was the minimum required to have the alkyltrimethylphosphonium salt well dissolved in water. *cmc* values for *n*ATMP·Br surfactants with *n* = 12, 14 and 16 at 25 ºC have been reported to go down from ~10 to ~0.6 mM for increasing values of *n* [12]. At the concentrations used for the preparation of their corresponding *n*ATMP·PGGA complexes (75, 50 and 10 mM, respectively), the surfactant must be in the form of micelles when it is made to contact with the polyelectrolyte. Unfortunately no data are

available for $n \geq 18$ but lower *cmc* values should be expected for longer alkyl chains. Although the higher temperatures used in the preparation of complexes for n = 18, 20 and 22 prevent from attaining a definite conclusion, it can be assumed that the surfactant is in the micellar state in these cases too.

Equimolecular amounts of polyacid and surfactant were mixed in all cases with higher concentration solutions used for lower values of n in order to optimize complex precipitation. In spite of that, yields were found to oscillate between 70 and 90% with the lower values corresponding to surfactants bearing shorter alkyl chains. The solubility behavior displayed by *n*ATMP·PGGA was found to be similar to that observed for the ionic complexes made of PGGA and alkyltrimethylammonium surfactants, *i.e.* they are soluble in organic solvents such as, chloroform, methanol, ethanol, TFE or DMSO but non-water soluble.

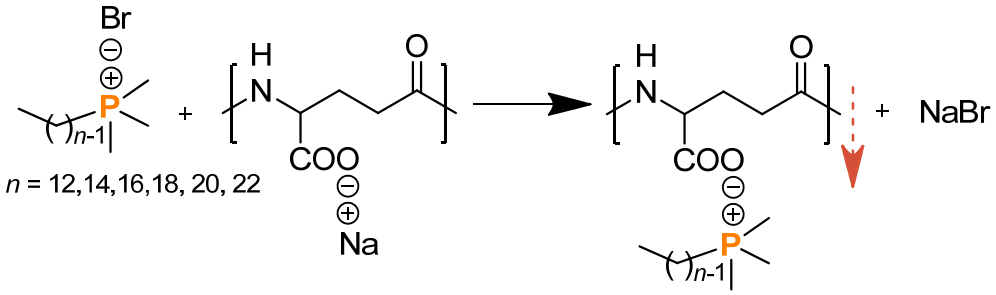

Scheme I. Coupling reaction of alkyltrimethylphosphonium bromides with Na·PGGA leading to *n*ATMP·PGGA ionic complexes.

The chemical constitution of the *n*ATMP·PGGA complexes was assessed by both FTIR and NMR spectroscopies. Infrared spectra showed characteristic bands at 3280 cm^{-1} (N-H stretching),1635 and 1540 cm^{-1} (Amide I and Amide II), the all three arising from the amide groups of PGGA, in addition to strong bands at 1590 and 1400 cm^{-1} attributed to the asymmetric and symmetric stretching modes of the carboxylate group. As expected bands at 2900, 2850 and 1470 cm^{-1} characteristic of alkyl groups were observed with their intensity steadily increasing with the length of the alkyl chain. On the other hand, conspicuous sharp bands

appearing at 990 and 715 cm^{-1} were attributable to the P-C stretching vibrations occurring in the alkylphosphonium groups. The FTIR spectra of Na·PGGA, 18ATMP·Br and 18ATMP·PGGA complex as well as those registered from the whole *n*ATMP·PGGA series are comparatively reproduced in the ESI file.

Table 1. Results for the preparation of *n*ATMP·PGGA complexes.

RMe_3P·Br	Complex	Mixing conditions[a]		Yield (%)	Composition[b]
		c (M)	*T* (ºC)		
-$C_{12}H_{25}$	12ATMP·PGGA	0.075	25	70	1.0:1.0
-$C_{14}H_{29}$	14ATMP·PGGA	0.05	25	80	1.1:1.0
-$C_{16}H_{33}$	16ATMP·PGGA	0.01	30	80	1.2:1.0
-$C_{18}H_{37}$	18ATMP·PGGA	0.01	45	85	1.2:1.0
-$C_{20}H_{41}$	20ATMP·PGGA	0.01	55	90	1.3:1.0
-$C_{22}H_{45}$	22ATMP·PGGA	0.01	65	90	1.3:1.0

[a]Molar concentration and temperature used for mixing.
[b]Molar ratio of *n*ATMP to PGGA in the complex as determined by NMR.

The ^{1}H NMR spectra of the *n*ATMP·PGGA complexes are compared in Fig. 1 with indication of peak assignments. Non assignable signals present in these spectra are negligible both in number and intensity, indicating therefore that complexes have been prepared with high purity. The ^{13}C NMR spectra, which are accessible in the ESI file, corroborated the chemical constitution of these complexes The composition of the complexes was estimated by comparing the area of the PGGA α-CH_2 signal appearing at 4.1 ppm with that of the signals located in the 1.2-1.5 ppm range which arise from the 2 to *n*-1 methylene protons contained in the phosphonium alkyl chain. The results afforded by this quantitative analysis revealed that the ratio of surfactant to polyacid in the complexes oscillated between 1.0 and 1.3 with values increasing with the length of the alkyl side chain (Table 1). Deviations from stoichiometry are very likely due to the coprecipitation of certain amounts of uncoupled surfactant, a process that should become more significant as the solubility of the ATMP·Br salt in water decreases.

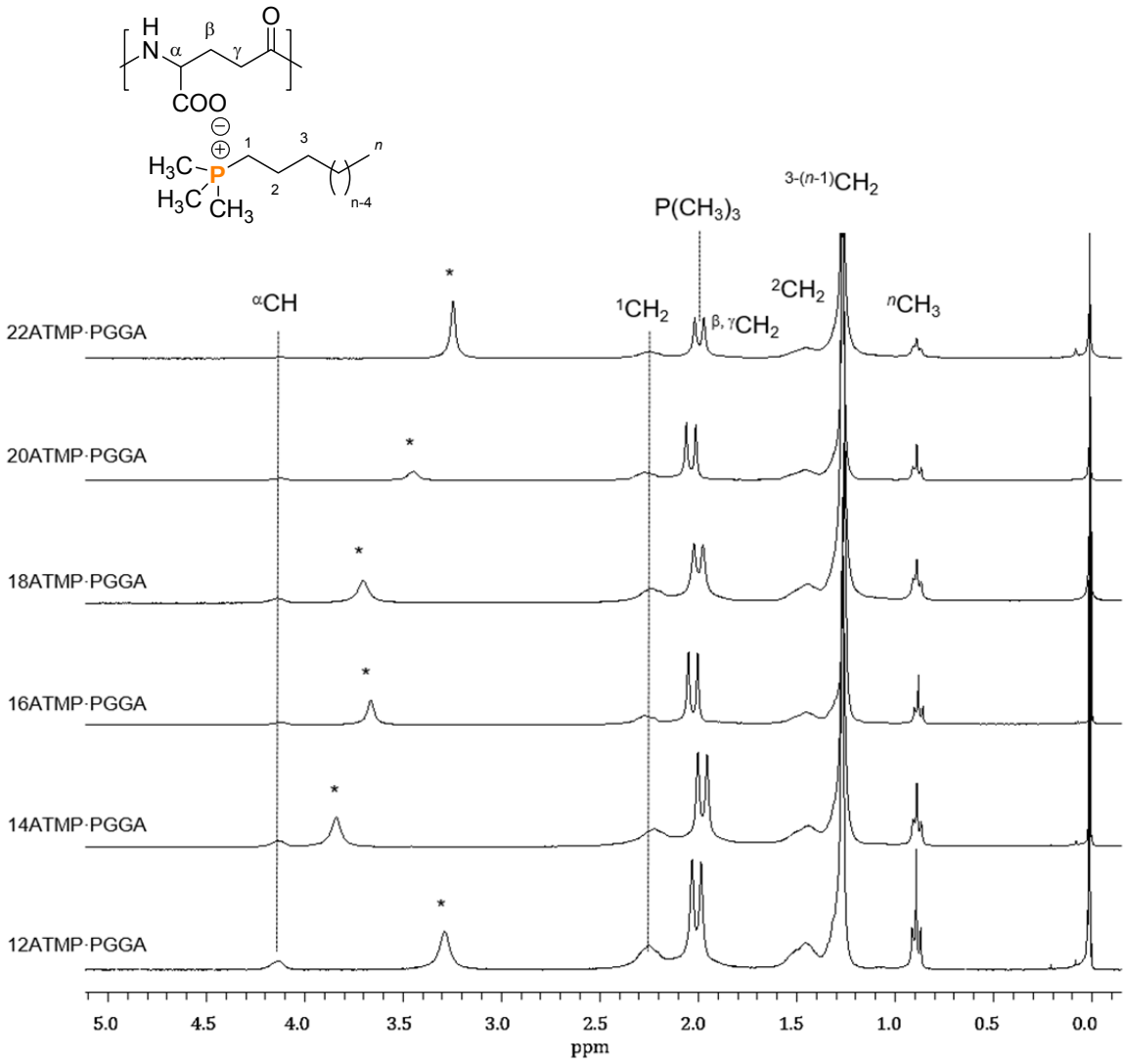

Fig. 1. Compared ^{1}H NMR spectra of *n*ATMP·PGGA in $CDCl_3$. (*) Peak arising from residual water.

3.2. Thermal properties of *n*ATMP·PGGA complexes.

The resistance to heat of *n*ATMP·PGGA complexes under an inert atmosphere was systematically examined by TGA. The recorded traces for the whole series together with their corresponding derivative curves are shown in Fig. 2, and the most significant thermal parameters are collected in Table 2. *n*ATMP·Br compounds are distinguished by displaying a

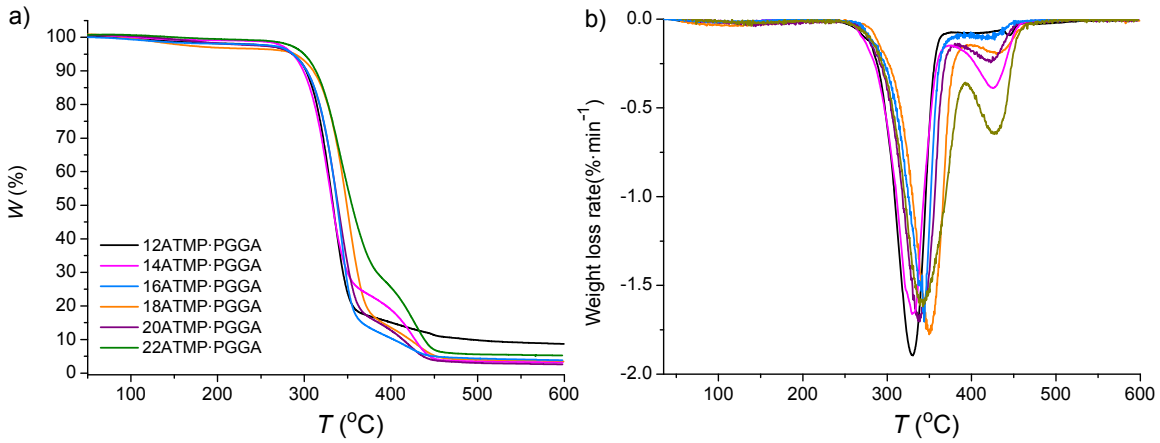

Fig. 2. Comparison of the TGA traces for the whole series of *n*ATMP·PGGA complexes (a) and their derivatives curves (b).

high thermal stability with onset degradation temperatures (ºT_d) around 400 ºC, a behavior that strongly contrasts with that shown by their *n*ATMA·Br analogs that start to decompose at temperatures between 200 ºC and 250 ºC [18]. On the other hand, PGGA is a relatively thermosensitive polymer that shows appreciable decomposition when heated above 200 ºC [19]. The TGA analysis of *n*ATMP·PGGA complexes revealed that these compounds follow a

Table 2. Thermal parameters of *n*ATMP·PGGA complexes.

n	**TGA**[a]			**DSC**[b]								
				1st Heating			Cooling		2nd Heating		
	$^{o}T_d$ (ºC)	$^{max}T_d$ (ºC)	*W* (%)	T_m (ºC)	ΔH_m (kcal·mol^{-1})	n_c	T_c (ºC)	ΔH_c (kcal·mol^{-1})	T_m (ºC)	ΔH_m (kcal·mol^{-1})	n_c
12	284	331/423	18/9	-	-	-	-	-	-	-	-
14	285	335/424	18/3	-	-	-	-	-	-	-	-
16	285	343/424	15/4	38	0.38	-	-	-	-	-	-
18	285	345/427	17/4	51	4.0	4.9	28	-2.5	35	2.3	2.9
20	286	345/427	19/5	63	5.8	6.9	47	-4.2	62	4.1	4.9
22	301	347/431	29/5	72	7.3	8.9	58	-6.0	72	5.6	6.9

[a] $^{o}T_d$ and $^{max}T_d$: onset and maximum rate decomposition temperatures; *W*: remaining weight at the end of each step.
[b] T_m and T_c: Melting and crystallization temperatures; ΔH_m and ΔH_c: melting and crystallization enthalpies; n_c: calculated number of crystallized methylene units.

thermal decomposition pattern which is the result of the reciprocal influence of their two components. In fact, upon gradual heating of the complexes, weight loss initiated at temperatures slightly below 300 ºC, which are values intermediate between those observed for PGGA and *n*ATMP·Br. Decomposition proceeded through two stages with maximum loss weight rates at the temperature ranges of 330-350 ºC and 420-430 ºC respectively, to leave less than 10% of residual weight and the end of the assay. It is noteworthy to recall that the *n*ATMA·PGGA complexes made from alkyltrimethylammonium surfactants display a similar thermal degradation pattern but with all decomposition temperatures displaced nearly 100 ºC lower [7,8]. The mechanism proposed for the pyrolysis of these complexes entailed the splitting of the complex ionic pair with concomitant generation of pyroglutamic acid at the first step followed by the decomposition of the surfactant counterpart at the second step [20]. Although no similar study has been undertaken in the present work for *n*ATMP·PGGA complexes, it does make sense to assume that both types of complexes should decompose through a similar mechanism. What is clearly evidenced anyway is the higher effect on PGGA thermal stability exerted by the alkylphosphonium surfactants when compared to their alkylammonium analogs.

The DSC study carried out on the *n*ATMP·PGGA complexes in this work has been addressed to identify the occurrence of reversible thermal transitions implying either melting or crystallization. It must be noticed that glass transition has never been observed for this kind of complexes previously reported either by us[7-10, 16,17] or by others.[15] In fact, no sign of slope change characteristic of *T*g was detected in the DSC traces of *n*ATMP·PGGA complexes registered over the -100 to 200 ºC range using different heating/cooling rates. For such purpose, samples were subjected to heating-cooling-heating cycles along the 25-120 ºC range since preliminary assays had revealed that all the observed heat exchange peaks were located between 30 ºC and 80 ºC. As it is shown in Fig. 3a, only complexes with $n \geq 16$ showed melting peaks, which appear at temperatures steadily increasing from 38 ºC (n =16) up to 72 ºC (n = 22). Upon cooling from 120 ºC, exothermal peaks characteristic of crystallization were observed

only for $n \geq 18$ with a supercooling of around 20 ºC. Their corresponding melting peaks were reproduced on the second heating traces at temperatures not far from those observed at first heating (Table 2). For illustrating graphically this transition the traces recorded for 22ATMP·PGGA are depicted in Fig. 3b and those recorded for n = 18 and 20 have been included in the ESI file.

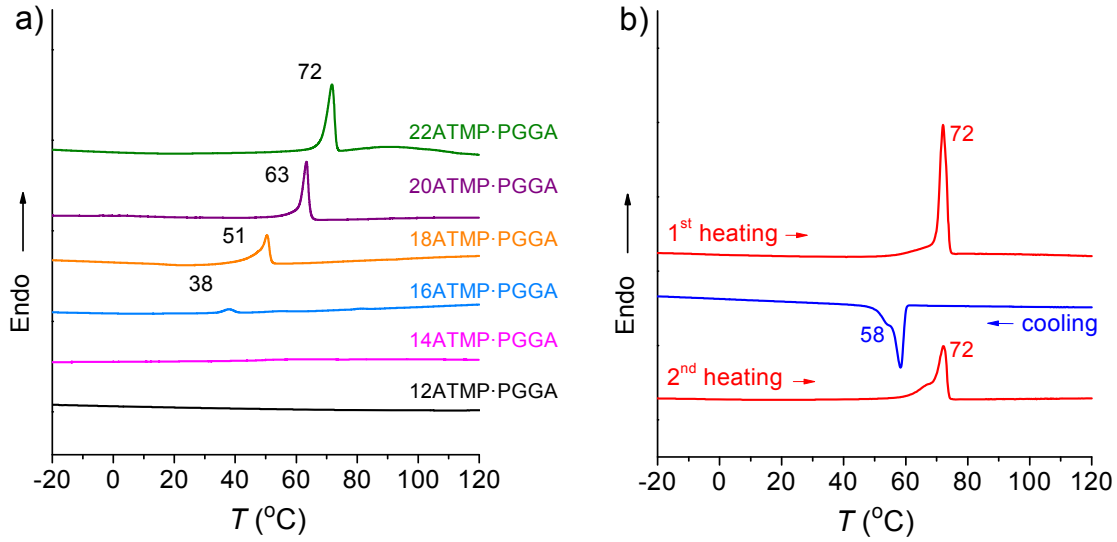

Fig. 3. First heating DSC traces of the whole set of *n*ATMP·PGGA complexes (a) and DSC traces of the 22ATMP·PGGA along the heating-cooling-heating cycle (b).

According to data previously reported for other PGGA ionic complexes bearing long alkyl side chains [7,8], the heat exchanges observed by DSC for *n*ATMP·PGGA must be related to the occurrence of a melting-crystallization process involving exclusively the paraffinic phase. The graphical representation of T_m against n reveals an almost linear dependence between these two variables with an increment of around 5 ºC for every carbon atom that is added to the alkyl chain (Fig. 4a). Also the variation of ΔH_m with n follows a similar dependence for the complexes showing crystallization except for n =16, which deviates down from linearity. The same trend was found for the melting of the complexes crystallized by cooling the heated samples although the enthalpy was in these cases about two kcal·mol^{-1} smaller (Fig. 4b). The

individual methylene (ΔH_m^{CH2}) and non-methylene (ΔH_m^0) contributions to the experimentally observed melting enthalpy are respectively given by the slope and the *y*-axis intercept at $n = 0$ of the linear ΔH_m-n plots [21]. The resulting values are around 0.8 kcal·mol^{-1}·CH_2^{-1} for ΔH_m^{CH2} and 10-12 kcal·mol^{-1} for ΔH_m^0 pointing that the crystallized alkyl chains must be packed in a pseudo-hexagonal array [22] and that only a fraction of the chain is included in the crystal phase. As it is seen in Table 2 and plotted in Fig. 4b, the amount of crystallized methylene units in crystallized *n*ATMP·PGGA samples oscillates between 3 and 9 (corresponding to chain fractions between 17% and 42%) depending on chain length and crystallization conditions. The trend observed for crystallinity and crystallizability in *n*ATMP·PGGA as the length of the alkyl chain changes is a feature of general application to all the comb-like PGGA derivatives studied

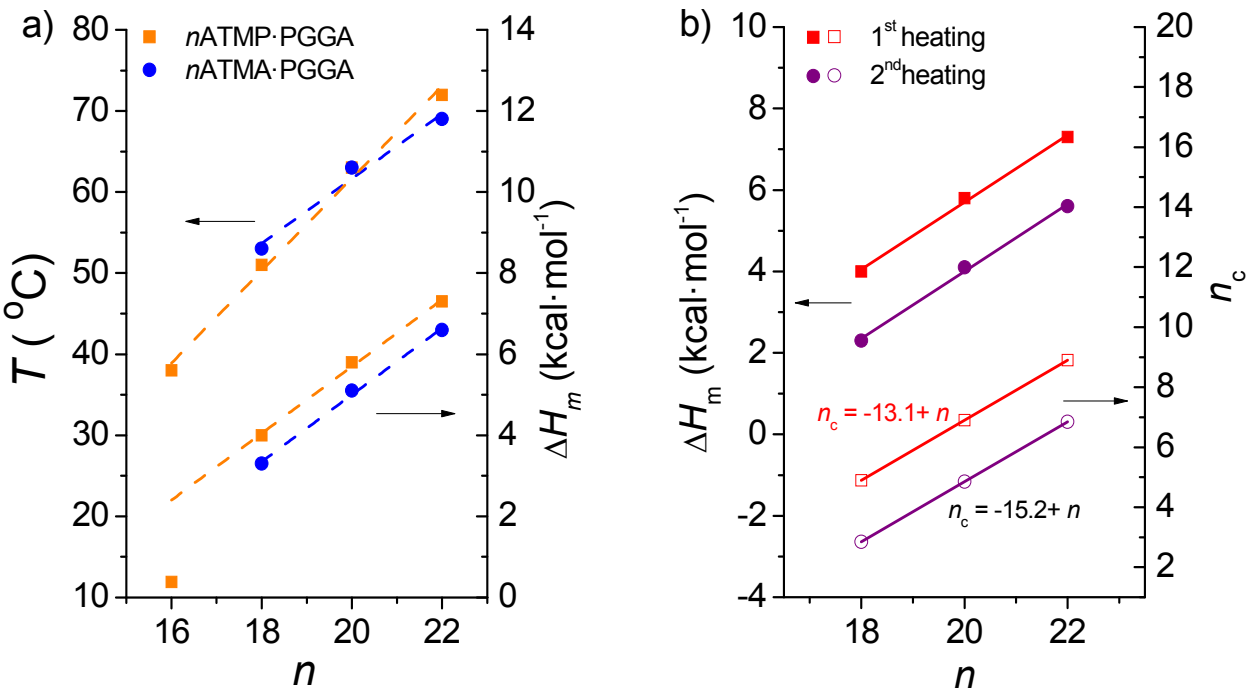

Fig. 4. a) Melting temperatures and enthalpies experimentally observed on the heating DSC traces recorded from pristine samples of *n*ATMP·PGGA and *n*ATMA·PGGA for n= 16, 18, 20 and 22. b) ΔH_m and number of crystallized methylenes (n_c) of 18, 20 and 22ATMP·PGGA complexes against the number of carbons contained in the alkyl chain for both pristine samples and samples crystallized from the melt.

to date including ionic-complexes [7,8,10] and poly(α-alkyl γ-glutamate)s as well [23]. For comparison, the DSC data reported for the *n*ATMA·PGGA series have been also plotted in Fig. 4a. As it can be seen the behavior of the two series regarding both melting temperatures and enthalpies are very similar although slightly higher values are invariable found for the *n*ATMP·PGGA complexes.

3.3. Supramolecular structure of *n*ATMP·PGGA complexes

The *n*ATMP·PGGA complexes have a comb-like architecture with a strongly marked amphiphilic constitution. The PGGA polypeptide chain including the attached carboxylate-phosphonium ionic pairs composes the hydrophilic part whereas the hydrophobic part is made of the pending long linear alky side chains. According to what has been repeatedly reported for other similar systems [7,8,10], the precipitation of these complexes from water taking place in situ as they are formed upon mixing their components is expected to happen through a self-assembling process. In fact, X-ray diffraction of the *n*ATMP·PGGA precipitates produced discrete light scattering characteristic of a well-organized material. The SAXS and WAXS

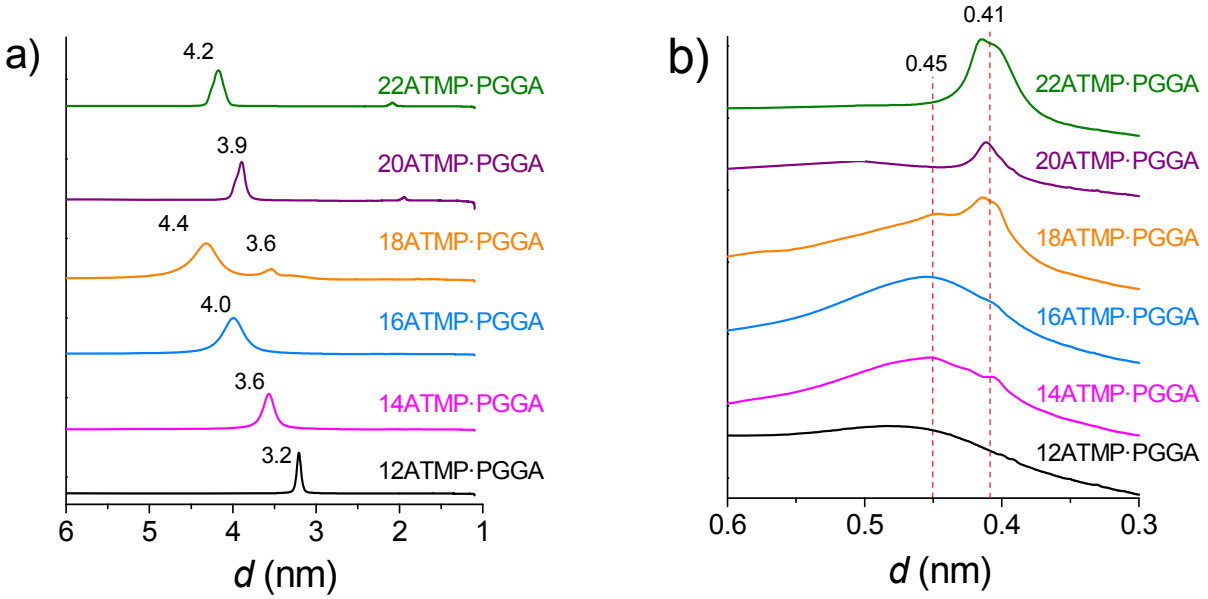

Fig. 5. XRD profiles recorded at room temperature from *n*ATMP·PGGA in the SAXS (a) and WAXS regions (b).

profiles recorded from the complexes are compared in Fig. 5 for the whole series. In the small-angle region (Fig. 5a), a strong peak corresponding to a spacing ranging between 3 and 5 nm is conspicuously observed for all the complexes, which is accompanied by a second minor one for the exceptional case of 18ATMP·PGGA. In line with the study carried out earlier on other ionic complexes of PGGA, these peaks appearing at low angles are interpreted as arising from theperiodical spacing of a structure made of alternating polypeptidic and paraffinic layers with a window that steadily increases with the length of the alkyl side chain. In fact, the plot of the long spacing (*L*) values measured by SAXS against *n* (Fig. 6) reveals that the periodicity of the layered structure varies almost linearly with *n* along the whole *n*ATMP·PGGA series but showing an abrupt discontinuity at *n* = 18. The *L*-*n* straight line fitting the complexes with *n* = 22, 20 and 18 (lower *L* value) displays a positive slope of ~0.15 nm·CH_2^{-1} whereas complexes with *n* =12, 14, 16 and 18 (higher *L* value) fit in a straight line that is displaced to higher *L* values and is inclined ~0.2 nm·CH_2^{-1}. Approximately the same *L*-intercept at *n* = 0 results for the two lines with a value of 0.8-0.9 nm which is interpreted as the thickness of the polypeptidic layer with the trimethylphosphonium groups therein included. No experimental data supporting a plausible explanation for the function discontinuity observed in this plot have been attained. A modification in the supramolecular arrangement of the complexes entailing a change in tilting or/and interdigitation of the alkyl side chains could be the reason for the observed jump. Also the presence of crystallinity detected for *n* ≥ 18 could be invoked to explain the *L* contraction undergone by these complexes. The dual *L* value displayed exclusively by *n* = 18 would indicate the occurrence of more than one structure or phase for the specific case of the 18ATMP·PGGA complex. It should be noticed that this behavior is also displayed by complexes made of hyaluronic acid and alkyltrimethylphosphonium surfactants (unpublished results) whereas a single straight line is found when complexes are made of alkyltrimethylammonium surfactants for both PGGA and hyaluronic acid. It seems therefore that it is the replacement of nitrogen by phosphorus that is behind the observed difference.

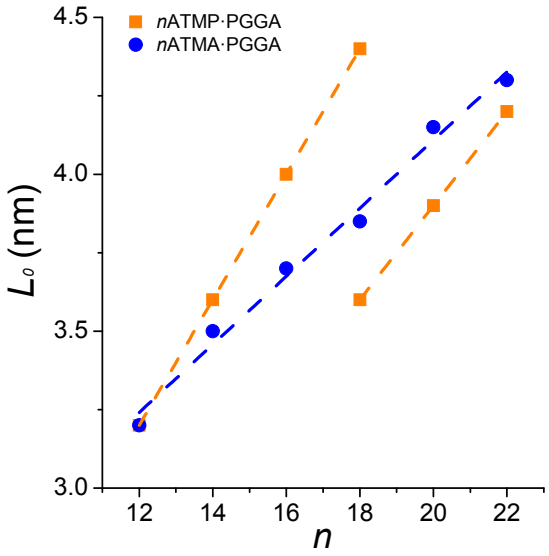

Fig. 6. Interlayer spacings observed at room temperature for *n*ATMP·PGGA as a function of *n*. Data reported for the *n*ATMA·PGGA [8] have been included for comparison.

The XRD data collected in the WAXS region afforded additional distinguishing structural information between the two groups of complexes (Fig 5b). The profiles recorded for 20ATMP·PGGA and 22ATMP·PGGA show a discrete peak at ~0.41 nm (d_{100}) characteristic of a paraffinic phase crystallized in a pseudo-hexagonal array of chains separated to one another by an average distance of about 0.47 nm (a_0). On the contrary, a broad signal characteristic of amorphous scattering and centered around 0.45 nm is the most prominent feature observed on the profiles produced by complexes with n = 12, 14 and 16. The WAXS profile of 18ATMP·PGGA show both discrete and diffuse scattering with comparable intensities revealing that crystallized as well as non-crystallized paraffinic material must be present in this complex in similar amounts.

No evidence on the conformation adopted by the polypeptide chain in the *n*ATMP·PGGA complexes is provided in this paper. Unfortunately, the information that could be provided by X-ray diffraction is probably masked by the strong scattering arising from the layered structure. The tendency of optically pure PGGA to be arranged in a helix is known for long. It was Rydon

[24] who first put forward a helical conformation of α-helix type for PGGA in the un-ionized state, a proposal that has been recently confirmed by molecular dynamics studies [25]. Nevertheless, on the basis of dichroic infrared analysis carried out on 18ATMA·PGGA [8], it was found that the conformation most probably adopted by PGGA in this kind of ionic complexes is a slightly folded conformation not far from the β-form of polypeptides, in which the carboxylate side groups become conveniently distributed in the space to allow an efficient packing of the alkyl side chains [8]. In the absence of any opposing evidence, there are reasons to assume that this conformation must be present in the *n*ATMP·PGGA too. The thickness that is estimated for the polypeptidic layer would be rather small to accommodate an α-helix, and the racemic composition of the PGGA used for building these complexes is in principle incompatible with any regular helical arrangement.

On the basis of the structure previously reported for other comb-like ionic complexes of PGGA [7,8] and with the support of the XRD results described above, a model may be proposed for the layered structure of *n*ATMP·PGGA which is drawn in Fig. 7. This model is essentially identical to that proposed for *n*ATMA·PGGA with the difference that the trimethylammonium

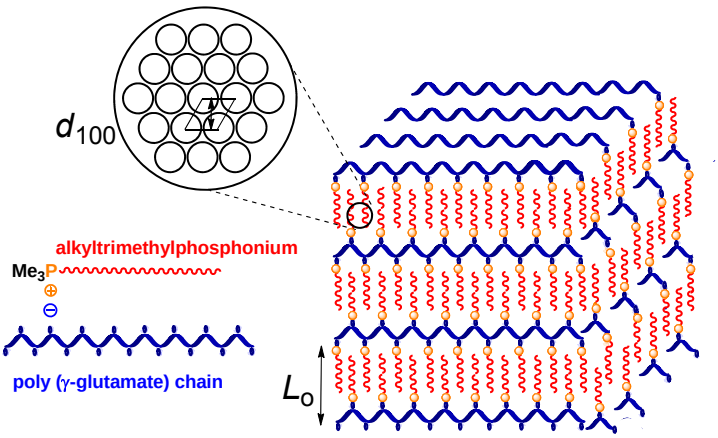

Fig. 7. Model for the layered structure adopted by *n*ATMP·PGGA complexes.

group is here replaced by the bulkier trimethylphosphonium one. It should be noted that although the alkyl chains are aligned with an orientation normal to the basal plane of the structure, they may be crystallized (*n* = 22 to 18) or not (*n* =18 to 12) and that in the former case, only a fraction of the chain will be in the crystalline state. Note also that the distance between carboxylate groups in one fully extended PGGA chain is ~0.6 nm whereas the longitudinally aligned alkyl chains are averagely separated by 0.47 nm or 0.45 nm depending whether they are crystallized or not. Fitting the paraffin phase to the polypeptidic layer will imply therefore a slight shrinkage of the PGGA chain in about 20% as well as deep interdigitation of the alkyl chains stemming from neighboring layers. The PGGA chains within the same layer would be connected to one another by hydrogen bonding the neighboring amide groups. The occurrence of liquid-crystal or semicrystalline phases for *n*ATMP·PGGA complexes at room temperature *n*ATMA·PGGA complexes corresponding to compositions for which the parafiinic phase was crystallized or not was supported by POM. Mosaic texture characteristic of a smectic structure was clearly identified for 12ATMP·PGGA whereas well-developed spherulitic morphologies indicative of semicrystalline material were observed for 20ATMP·PGGA and 22ATMP·PGGA. The textures exhibited by the complexes with *n* = 14, 16 and 18 were more difficult to interpret probably because they reflect the occurrence of more than one phase coexisting in the material at the temperature at which images were taken. A complete collection of POM pictures including the whole series of complexes is given in the ESI file.

3.4. Temperature effects on the structure of *n*ATMP·PGGA complexes.

The effect of temperature on the layered structure adopted by the *n*ATMP·PGGA complexes was examined by XRD at real time using synchrotron radiation. Samples were subjected to heating-cooling-heating cycles covering the 10 ºC to 120 ºC range at a heating/cooling rate of 10 ºC·min^{-1}. The spacings observed at the beginning and the end of each

run for every complex are compared in Table 3, and the charts showing the evolution of the scattering profile in both SAXS and WAXS regions for every 3 ºC of temperature change are

Table 3. X-ray diffraction data (in nm) of *n*ATMP·PGGA complexes recorded at different temperatures.

n	**SAXS**			**WAXS**		
	$L^{10ºC}$	$L^{120ºC}$	$L^{10ºC}$	$d_{100}^{10ºC}$	$d_{100}^{120ºC}$	$d_{100}^{10ºC}$
12	3.2	3.0	3.3	0.45	0.45	0.45
14	3.6	3.4	3.7	0.45 (0.41)	0.45	0.45
16	4.0	(3.7), 3.6	(3.9), 3.6	0.45, (0.41)	0.45	0.45
18	4.4 (3.6)	3.9, (3.3)	3.9, (3.4)	0.45, 0.41	0.45	0.45
20	3.9	3.8	3.9	0.41	0.45	0.41
22	4.2	4.0	4.1	0.41	0.45	0.41

L: interlamellar distance; d_{100}: interplanar spacing of the crystallized paraffinic phase; in parenthesis, values for very weak peaks.

included in the ESI file. General features observed in these X-ray thermodiffractograms are a decreasing trend of the periodical long spacing of the structure as temperature raised and an almost complete reversibility of the occurring changes after cooling. However, more or less significant differences were observed among the members of the series, which are consistent with the results obtained by DSC. It should be noticed that almost identical results were obtained for the two components of the extreme pairs, *i.e* 12ATMP·PGGA/14ATMP·PGGA and 22ATMP·PGGA/20ATMP·PGGA, whereas clear differences were evidenced between the two pairs. The charts for *n*= 12 and *n* = 22, which are taken as representatives of each pair, are shown in Fig. 9 and 10, respectively. The SAXS profiles recorded for 12ATMP·PGGA at 10 ºC show a sharp peak corresponding to a spacing of 3.2 nm that moves evenly down until 3.0 nm at 120 ºC and that reverses to near the initial value upon cooling (Fig. 8a). The WAXS scattering produced by this complex is completely insensitive to temperature effects so that the flat profile initially recorded is maintained invariable along the whole heating-cooling-reheating cycle (Fig. 8b). Exactly the same pattern of behavior was found for 14ATMP·PGGA with the initial SAXS peak appearing in this case at 3.6 nm and going down to 3.4 nm at 120 ºC. Conversely the

response to temperature of 22ATMP·PGGA was significantly different both in SAXS and WAXS (Fig. 9). The SAXS peak at 4.2 nm present at 10 ºC also moved slightly to down values but in this case with a jump taking place at the surrounding of 70 ºC (Fig. 9a), which is the melting temperature detected by DSC for this complex. The WAXS chart (Fig. 9b) shows how the 0.41 nm peak characteristic of the crystallized paraffinic phase disappears at the melting temperature and is then recovered after cooling down to the initial temperature. Exactly the same pattern of behavior was found for 20ATMP·PGGA with the initial SAXS peak appearing in this case at 3.9 nm and going down to 3.8 nm at 120 ºC.

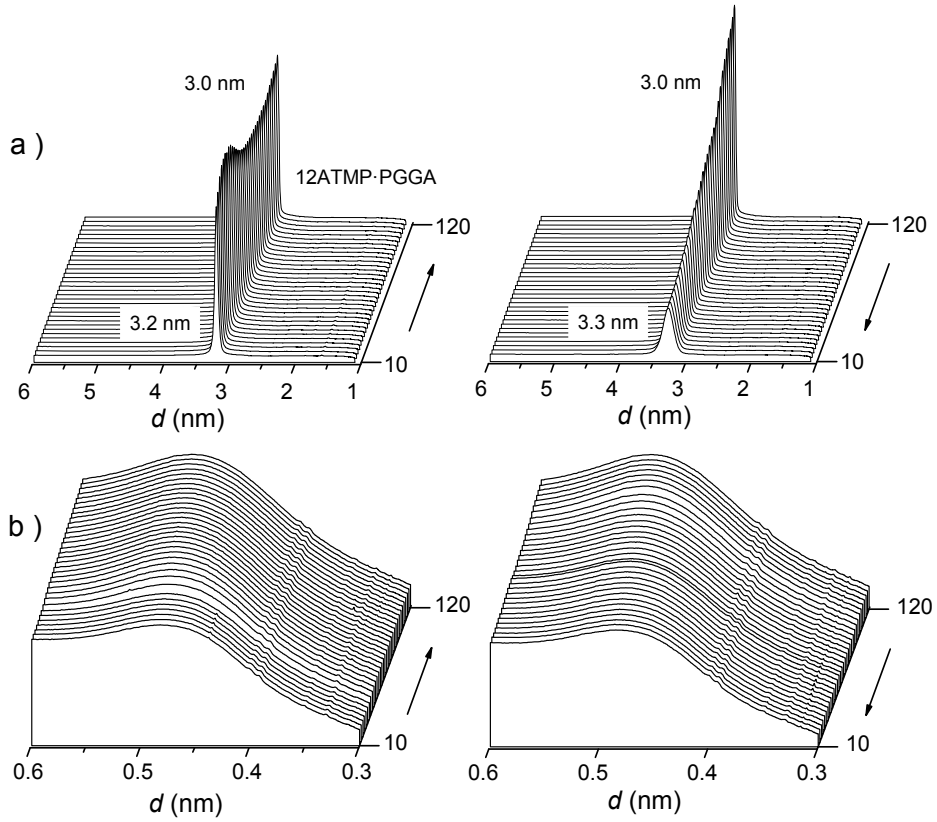

Fig. 8. SAXS (a) and WAXS (b) profiles of 12ATMP·PGGA at heating (left) and cooling (right).

The behavior observed for both 16ATMP·PGGA and 18ATMP·PGGA is more intricate not only due to the presence of significant amounts of both crystallized and non-crystallized

material. Furthermore the implication of more than two supramolecular arrangements in the heating-cooling process cannot be discarded. In these cases two peaks are observed in the SAXS profiles either from the beginning or after heating, and the discrete peak initially present in WAXS was not recovered after cooling the heated sample (see ESI file). Although reversible dimensional changes also happen for these intermediate complexes when they are subjected to heating and cooling, and a melting-crystallization process is in some extent also involved, the interpretation of such changes is not easy. A more detailed analysis by XRD in combination with calorimetric and polarizing optical microscopy should be made in order to achieve a sounded explanation for the structural transformations detected for these two complexes.

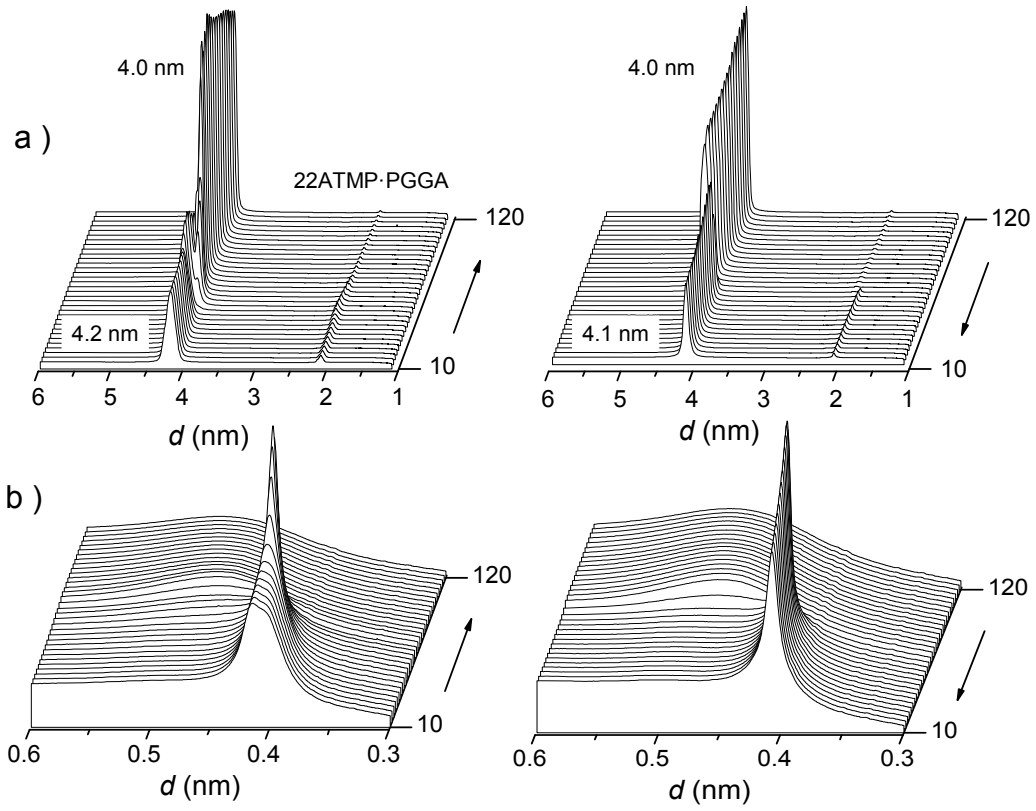

Fig. 9. SAXS (a) and WAXS (b) profiles of 22ATMP·PGGA at heating (left) and cooling (right).

3.5. Dissociation of *n*ATMP·PGGA complexes in aqueous environment and antimicrobial activity

The ionic nature of the *n*ATMP·PGGA complexes make them to be in thermodynamic equilibrium with their ionic components when they are in an aqueous environment. The intrinsic extent of the equilibrium for the different members of the series will be mainly determined by both the water solubility of the trimethylalkylphosphonium cation and the ability of PGGA to be homogeneously mixed with water either by partial swelling of sequentially charged segments or even by solubilization of the whole chain after sufficient ionization. The dissociation of the complexes upon incubation in water was estimated by measuring the absorbance at 208 nm as a function of time and the profiles obtained for the whole series along a period of seven days at pH 7.0 and 5.0 are represented in Fig. 10. It should be minded that both PGGA and the trimethylphosphonium cation are able to absorb at the applied wavelength so that the observed absorbance is due to the presence of the two ionic species. However absorptivity has essentially the same value for the two species which prevents to determine by this method the ratio at which they are present in the solution. Nevertheless, a comparative inspection of the results allows to state that a) Complex dissociation decreases with the length of the alkyl chain so that it becomes only significant for *n* values lower than 18. This is a much expected result given the strong dependence of surfactant solubility on *n*. b) For all complexes the amount of released ions is higher at pH 7.0 than at pH 5.0. This is a rather striking result since one could expect that a more protonated polyacid occurring at lower pH would facilitate the release of the organocation. However the ionization degrees at pH 5 and 7 of PGGA (pKa 2.27) are >99.9% and 99.9999% respectively so that the influence of ionization on the release of the surfactant at any of these two pH's may be considered negligible. Furthermore the visual inspection of the complex film after incubation revealed more apparent changes at pH 7 than at pH 5 (an illustrative picture has been included in the ESI document). c) The maximum dissociation extent happens for 12ATMP·PGGA at pH 7.0 but the ionic concentration in water is smaller than 10% of the initial complex concentration.

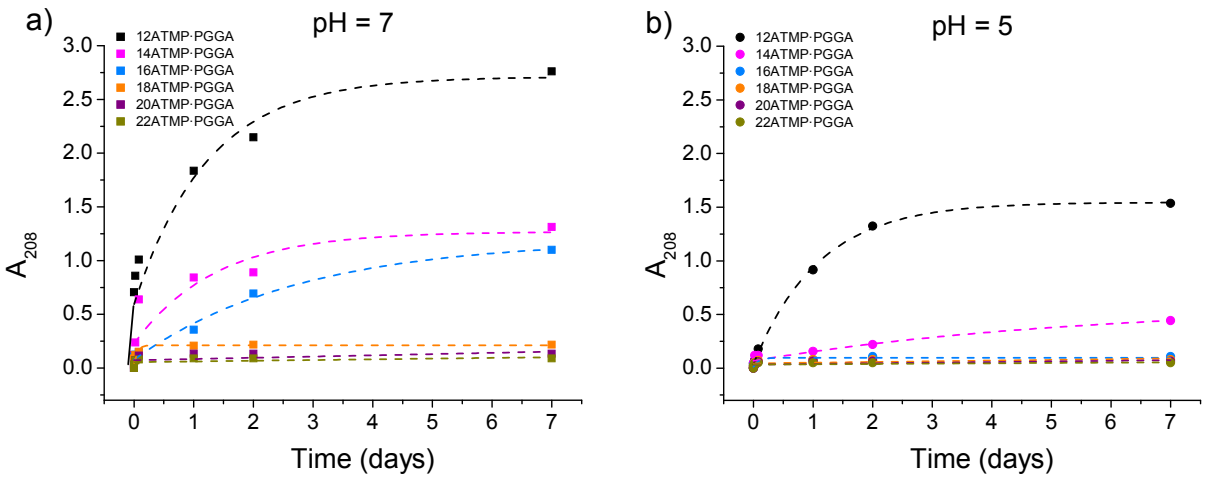

Fig.10. Dissociation of *n*ATMP·PGGA complexes in water at pH 7 (a) and 5 (b).

The biocide activity of organic quaternary salts is a well-known fact that has been widely reported and that is currently exploited for building a diversity of materials and formulations with bactericide or/and fungicide properties [26]. Organophosphonium salts are particularly efficient in this regard and their use in the preparation of polymeric materials with biocide activity has been accomplished by different approaches that include blending, surface attachment or covalent incorporation into the polymer chain either in the backbone or as pending side groups [27-30]. Given the capacity of the *n*ATMP·PGGA complexes to render consistent films suitable for coating or packaging, it was interesting to explore the antimicrobial activity of such films. For this preliminary study, two common bacteria, Gram-negative *E. coli* and Gram-positive *S. aureus* at pH 5 and pH 7 were selected for the assays, and two methods differing in the way that the active agent contacts the bacteria were applied. The bacterial growth inhibition estimated by counting of the colonies along time either visually or by turbidimetry was taken as a measure of the biocide activity.

In the first method, the microorganism growth evolution with time was followed while the complex film was immersed in the bacteria suspension. Results obtained for the whole series and for neat PGGA are compared in Fig.11. Taken the control (assay carried out in absence of polymer) as reference it becomes evident that at the scale of time used, complexes for $n \geq 20$ and also PGGA are fully inactive under the two assayed pHs, and that 18ATMP·PGGA shows only weak activity against *E. coli* at pH 5. On the contrary, complexes for n = 12, 14 and 16 display a general strong antibacterial activity at pH 7 with almost total growth inhibition after 24 h of incubation except for the case of 16ATMP·PGGA that needed several days for a complete disappearance of the colonies. The activity of these complexes at pH 5.0 was in general lower than a pH 7.0 and much higher against *S. aureus*.

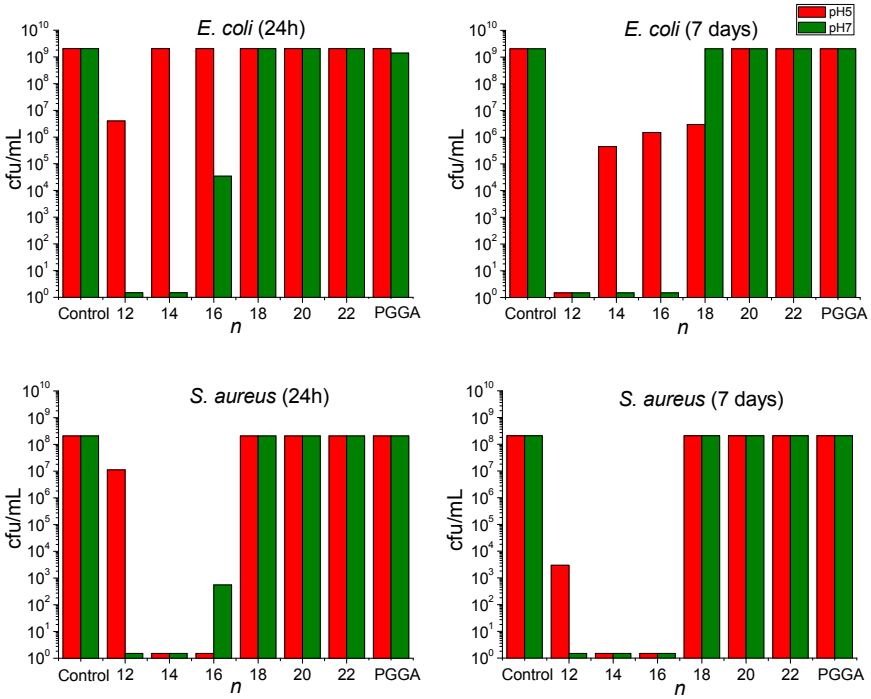

Fig. 11. Bactericide activity against *E. coli* and *S. aureus* of *n*ATMP·PGGA films after incubation for 24 h and 7 days at the two indicated pHs. The antimicrobial effectiveness is expressed as the visually estimated concentration of colonies forming units.

The results obtained after application of the second method are shown in Fig.12. In this case, the direct contact of films with bacteria was avoided and the biocide activity was measured for the species leached from *n*ATMP·PGGA films to the supernatant after incubation for five days. The resulting microbial activity was very similar to that obtained by the first method but the general behavior was even more systematic. The supernatants recovered from *n*ATMP·PGGA complexes with $n \leq 16$ were fully efficient in killing the bacteria so total inhibition was effective since the beginning. For $n = 20$ and 22, the curves were similar to those obtained for the control displaying the typical growth evolution in three or four phases, (lag, exponential, stationary and death), which indicates the total inactivity of these complexes against the two assayed bacterial species. The behavior displayed by 18ATMP·PGGA was somewhat erratic; in this case a strong antimicrobial activity was shown except when tested against *E. coli* at pH 5 which is in disagreement with results obtained in the former assay.

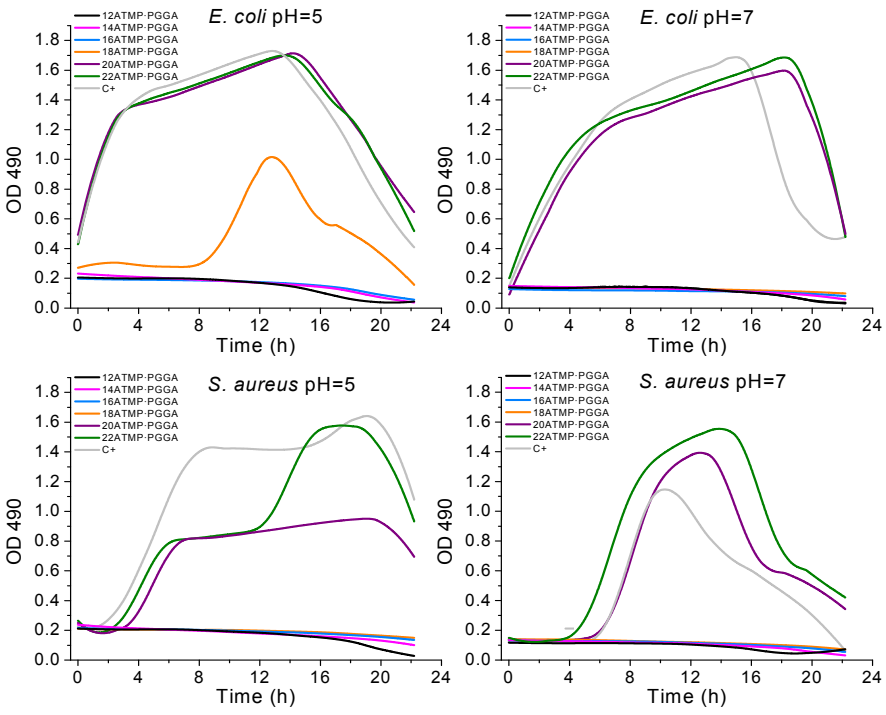

Fig. 12. Bactericide activity of the supernatant recovered from *n*ATMP·PGGA films incubated for 5 days at the two indicated pHs. The antimicrobial activity was measured along 24 h and is expressed as the reduction in optical absorption at 490 nm.

The unquestionable conclusion that can be drawn from the results obtained from the biocide assays is that *n*ATMP·PGGA complexes with short alkyl side chains (*n* = 12, 14 and 16) display strong antimicrobial activity against both Gram-positive and Gram-negative bacteria. Such activity must be associated to the organophosphonium counterpart which is partially delivered to the aqueous environment upon incubation. It can be inferred therefore that the bactericide activity of *n*ATMP·PGGA complexes is eventually determined by the water solubility of the surfactant implied in each case, and in less extent by the influence of incubation conditions on the stability of the complex.

4. Conclusions

Comb-like ionic complexes (*n*ATMP·PGGA) could be successfully prepared by mixing aqueous solutions of PGGA and alkyltrimethylphosphonium bromides with linear alkyl chains containing even numbers of carbon atoms ranging from 12 to 22. The ionic composition of the complexes was nearly stoichiometric with deviations being larger for longer alkyl chains. The complexes were non-soluble in water but readily soluble in organic solvents. These complexes based on organophosphonium cations displayed excellent thermal stability with onset decomposition temperatures near to 300 ºC, which are about 100 ºC higher than those reported for similar complexes made from alkyltrimethylammonium surfactants. *n*ATMP·PGGA complexes are arranged in a amphiphilic structure that follows the same biphasic layer pattern described for their ammonium analogs and displays a similar trend for the crystallization of the paraffinic phase. However, higher melting enthalpies were observed for these complexes indicating that a larger fraction of the polymethylene segment is able to crystallize when the alkyl chain is attached to the phosphorous atom. The response of the *n*ATMP·PGGA complexes to temperature changes consists of a reversible shortening of the layer periodicity in about 5%

of the original value upon heating from the 10 to 120 ºC, which is exactly opposite to what happens in the ammonium complexes. Finally it has been evidenced that the *n*ATMP·PGGA with *n* = 12, 14 and 16 display strong bactericide activity as a consequence of the weak release of the alkyltrimethylphosphonium species that take place in such complexes when incubated in an aqueous environment. The combination of this property with the ability to form films by either hot-pressing or casting confers on these complexes potential for being used in active coating or packaging applications.

Acknowledgements

This work received financial support from MCINN (Spain) with Grant MAT2012-38044-C03. Portions of this research were carried out at the BL11 line of ALBA synchrotron (Cerdanyola del Vallès, Barcelona, Spain) with the invaluable support of Dr. Christina Kamma-Lorger. Authors are indebted to Dr. Marta Fernández-García (ICP, CSIC, Madrid) for useful comments and helpful guidance of the biocide assays. Thanks also to the MICINN for the Ph.D. grant awarded to Ana Gamarra Montes.

References

[1] S. Muñoz-Guerra, M. García-Alvarez, J.A. Portilla-Arias, J. Renew. Mater. 1 (1) (2013) 42–60.

[2] E.T. Kubota H, Fukuda H, H. Takebe, Pat. Number US5118784. Meiji Seika Kabushiki Kaisha. (1992).

[3] D.T. Shah, S.P. McCarthy, R.A. Gross, Pat. Number US5378807-A. Univ Massachusetts Lowell (UMAC-C) (1995).

[4] M. Kunioka, K. Furusawa, J. Appl. Polym. Sci. 65 (10) (1997) 1889–1896.

[5] T. Akagi, M. Higashi, T. Kaneko, T. Kida, M. Akashi, Biomacromolecules 7 (1) (2006) 297–303.

[6] M. Antonietti, J. Conrad, A. Thuenemann, Macromolecules 27 (21) (1994) 6007–6011.

[7] M. García-Álvarez, J. Álvarez, A. Alla, A. Martínez de Ilarduya, C. Herranz, S. Muñoz-Guerra, Macromol. Biosci. 5 (1) (2005) 30–38.

[8] G. Pérez-Camero, M. García-Álvarez, A. Martínez de Ilarduya, C. Fernández, L. Campos, S. Muñoz-Guerra, Biomacromolecules 5 (1) (2004) 144–152.

[9] A. Tolentino, A. Alla, S. Muñoz-Guerra, Eur. Polym. J. 48 (11) (2012) 1838–1845.

[10] A. Tolentino, S. León, A. Alla, A. Martínez de Ilarduya, S. Muñoz-Guerra, Macromolecules 46 (4) (2013) 1607–1617.

[11] A. Tolentino, A. Alla, A. Martínez de Ilarduya, S. Muñoz-Guerra, Int. J. Biol. Macromol. 66 (2014) 346–353.

[12] A. Gamarra, L. Urpí, A. Martínez de Ilarduya, S. Muñoz-Guerra, Phys. Chem. Chem. Phys. 14 (2017) 4837-4845.

[13] W. Xie, R. Xie, W.P. Pan, D. Hunter, B. Koene, L.S. Tan, R. Vaia, Chem. Mater. 14 (11) (2002) 4837–4845.

[14] A. Kanazawa, T. Ikeda, T. Endo, Antimicrob. Agents Chemother. 38 (5) (1994) 945–952.

[15] E.A. Ponomarenko, A.J. Waddon, D.A. Tirrell, W.J. Macknight, Langmuir 12 (5) (1996) 2169–2172.

[16] A. Tolentino, A. Alla, A. Martínez de Ilarduya, S. Muñoz-Guerra, Carbohydr. Polym. 86 (2) (2011) 484–490.

[17] A. Tolentino, A. Alla, A. Martínez de Ilarduya, S. Muñoz-Guerra, Carbohydr. Polym. 92 (1) (2013) 691–696.

[18] A. Kanazawa, O. Tsutsumi, T. Ikeda, Y. Nagase, J. Am. Chem. Soc. 119 (33) (1997) 7670–7675.

[19] H. Kubota, Y. Nambu, T. Endo, J. Polym. Sci. Part A Polym. Chem. 33 (1) (1995) 85–88.

[20] J.A. Portilla-Arias, M. García-Álvarez, A. Martínez de Ilarduya, S. Muñoz-Guerra, Polym. Degrad. Stab. 92 (10) (2007) 1916–1924.

[21] E.F. Jordan, D.W. Feldeisen, A.N. Wrigley, J. Polym. Sci. Part A-1 Polym. Chem. 9 (7) (1971) 1835–1851.

[22] M.G. Broadhurst, Phys. Chem. 66A, No.3 (3) (1962) 241–249.

[23] M. Morillo, A. Martínez de Ilarduya, S. Muñoz-Guerra, Macromolecules 34 (22) (2001) 7868-7875.

[24] H.N. Rydon, J. Chem. Soc. (1964) 1328–1333.

[25] D. Zanuy, C. Alemán, S. Muñoz-Guerra, Int. J. Biol. Macromol. 23 (3) (1998) 175–184.

[26] A. Mu, M. Fernández-García, Prog. Polym. Sci. 37 (2012) 281–339.

[27] A. Kanazawa, T. Ikeda, T. Endo, J. Polym. Sci. Part A Polym. Chem. 31 (2) (1993) 3031–3038.

[28] Y. Xue, H. Xiao, Y. Zhang, Int. J. Mol. Sci. 16 (2) (2015) 3626–3655.

[29] A. Popa, M. Crisan, A. Visa, G. Ilia, Brazilian Arch. Biol. Technol. 54 (1) (2011) 107–112.

[30] T. Qiu, Q. Zeng, N. Ao, Mater. Lett. 122 (2014) 13-16.